

Topological Effects on Cyclic Co-Poly(Ionic Liquid)s Self-Assembly

Qingquan Tang,* Hao Ren, Zdravko Kochovski, Lisheng Cheng, Ke Zhang, Jiayin Yuan,* and Weiyi Zhang*

Topological geometry of poly(ionic liquid)s (PILs), such as brush-like, knot-like, hyperbranched and randomly coiled, often exerts a strong influence on their self-assembly behaviors. As a primary topological form, the cyclic topology-derived effects have not been investigated on PILs, which concerns synergy of charges and zero chain end. Herein, linear and cyclic poly(ionic liquid) copolymers (co-PILs) with randomly distributed counter anions of $B(Ph)_4^-$ and Br^- by a template method in combination with a follow-up partial anion exchange is prepared. The self-assembly phenomena of linear and cyclic co-PILs are studied in selective solvents, where the hydrophobic counter anions $B(Ph)_4^-$ and hydrophilic counter anions Br^- aggregated to form cores and corona in the assembled nanospheres, showing the average size of cyclic co-PILs nanospheres is 46.2% smaller (≈ 120 nm) than linear co-PILs nano-assemblies (≈ 176 nm). Based on the CGMD simulations, the authors speculate that the spherical aggregates are formed by transitioning from micelles with gradient block-like structures, which formed by enriched hydrophobic counter anions in the core and enriched hydrophilic counter anions in the corona. These results indicate a novel synergy of topology effects and dynamic anion movements, as revealed by cyclic co-PIL self-assembly in this work.

1. Introduction

Poly(ionic liquid)s (PILs), as polymers composed of repeating ionic liquid moieties, inherit some physicochemical properties both from ionic liquids and polymers. They are useful materials platforms for versatile applications, e.g. biosensors, catalysis, actuators, polymer electrolytes, and self-assembled nanoparticles.^[1–7] Self-assembly behaviors of PILs were influenced by numerous parameters, such as chemical compositions, counterions, coulombic interactions, topologies, etc.^[1–5] For instance, hyperbranched,^[8] star-like,^[9] and brush-shaped^[10] PILs were investigated to elucidate their topology/self-assembly relationships. These PILs with differed topologies bear adequate chain ends in comparison with linear ones, which decrease their entanglements heavily.² However, self-assembly behaviors of PILs without chain ends, such as cyclic PILs, are largely unknown.

Q. Tang, H. Ren
College of Materials Science and Engineering, State Key Laboratory of New Textile Materials & Advanced Processing Technology
Wuhan Textile University
Wuhan 430200, China
E-mail: qqtang@wtu.edu.cn

Z. Kochovski
Department for Electrochemical Energy Storage
Helmholtz-Zentrum Berlin für Materialien und Energie
Hahn-Meitner-Platz 1, 14109 Berlin, Germany

L. Cheng
College of Mechanical and Electrical Engineering
Beijing University of Chemical Technology
Beijing 100029, China

L. Cheng
State Key Laboratory of Organic-Inorganic Composites
Beijing University of Chemical Technology
Beijing 100029, China

K. Zhang
Laboratory of Polymer Physics and Chemistry, Beijing National Laboratory for Molecular Sciences, Institute of Chemistry
The Chinese Academy of Sciences
Beijing 100190, China

K. Zhang
University of Chinese Academy of Sciences
Beijing 100049, China

J. Yuan
Department of Materials and Environmental Chemistry
Stockholm University
Stockholm 10691, Sweden
E-mail: jiayin.yuan@mmk.su.se

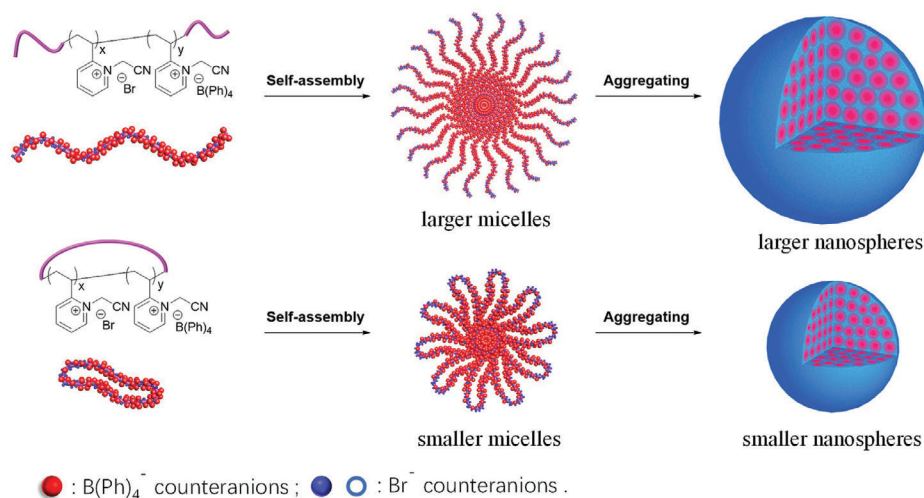
W. Zhang
College of Materials Science and Engineering, State Key Laboratory for Modification of Chemical Fibers and Polymer Materials
Donghua University
Shanghai 201620, China
E-mail: wyzhang@dhu.edu.cn

W. Zhang
State Key Laboratory of Molecular Engineering of Polymers
Fudan University
Shanghai 200438, China

 The ORCID identification number(s) for the author(s) of this article can be found under <https://doi.org/10.1002/macp.202200134>

© 2022 The Authors. Macromolecular Chemistry and Physics published by Wiley-VCH GmbH. This is an open access article under the terms of the Creative Commons Attribution License, which permits use, distribution and reproduction in any medium, provided the original work is properly cited.

DOI: 10.1002/macp.202200134



Scheme 1. Schematic illustration of the speculated self-assembly process of linear (top) and cyclic (bottom) poly(ionic liquid) copolymers. Note: in the micelles, the B(Ph)_4^- dominant core contains a small fraction of Br^- anions, and the Br^- dominant corona area contains a small fraction of B(Ph)_4^- anions.

Conventionally, the loss of chain ends endows cyclic neutral polymers with distinctive self-assembly behaviors. For example, cyclic polystyrene-*block*-poly(ethylene oxide)s demonstrated 30% decrease in domain spacings when self-assembled into ordered patterns in a thin film, in comparison with linear diblock copolymers precursors of similar molecular weights.^[11] Alternatively, well-defined cylindrical nanotubes were creatively constructed by self-assembly of cyclic brush copolymers, where cyclic polymer backbones were decorated with randomly distributed polystyrene and polyisoprene mixtures.^[12] In that work, the distinct self-assembly behaviors of cyclic amphiphilic diblock copolymers could be ascribed to the stretch of polymer chains restricted by the loop, which resulted in a smaller hydrodynamic radius of micellar assembly, in comparison with the linear analogues.^[13] Intriguingly, higher thermal stability and greater tolerance of cyclic assemblies towards salt additives were observed in contrast with the corresponding linear ones, due to the smaller effective volume and the lack of inter-micelle bridges.^[14–16] Nevertheless, because the “polyelectrolyte effect” hampers the direct synthesis of cyclic PILs by cyclizing linear PILs based on the ring-closure method,^[17–19] the self-assembly of cyclic PILs has not been explored before.

Recently, we reported a post-modification method to prepare cyclic PILs via applying neutral cyclic polymers as templates, since under the same conditions the ring-closure cyclization of PILs is hampered by the “polyelectrolyte effect”, for which polyelectrolyte backbones are stretched in dilute solution due to the electrostatic repulsion of neighboring charged units.^[20] Upon circumventing the “polyelectrolyte effect” by using neutral cyclic polymers as intermediate, charged cyclic ones can be obtained from quaternization reactions and the following anion exchange reactions. Interestingly, amphiphilic linear poly(ionic liquid) copolymers (co-PILs) with randomly distributed counter anions were reported to self-assemble into nanoparticles in selective solvents without the requirement of adopting a well-structured block copolymers.^[21,22] However, there is still a lack of research on the self-assembly of cyclic co-PILs.

Herein, we report a facile method to prepare cyclic amphiphilic random co-PILs and compare their self-assembly behaviors with linear ones (**Scheme 1**). Linear and cyclic co-PILs with randomly distributed counter anions of Br^- and B(Ph)_4^- were synthesized by quaternization reaction of linear and cyclic P2VP and then the subsequent partial anion-exchange. Counter anion of B(Ph)_4^- was chosen to realize the partial anion-exchange, owing to its high hydrophobicity coming from the bulky aromatic groups.^[23,24] This strategy avoided complicated synthetic processes and purification steps that are usually involved in the preparation of amphiphilic block copolymers, in which well-defined blocks were required for phase separations.^[25] As such, cyclic PILs bearing randomly distributed hydrophobic/hydrophilic counter anions can be readily synthesized and next employed to perform self-assembly in selective solvents. The self-assembly behaviors between linear and cyclic co-PILs were studied, and both exhibited similar bulky spheric morphologies, while a smaller size of cyclic co-PILs-derived nanoassemblies was found than that of linear ones, as evidenced by various characterizations and computational simulations through molecular dynamics.

2. Results and Discussion

Linear and cyclic co-PILs were synthesized according to our previously reported literature (Scheme S1).^[20] Linear poly(2-vinylpyridine) (LP2VP) with a controlled molecular weight and a polydispersity index of $M_n = 14100$ and $\text{PDI} = 1.13$, respectively, was prepared by standard reversible addition-fragmentation chain transfer (RAFT) polymerization technique (Figure S1, Supporting Information, black). The corresponding cyclic P2VP (CP2VP) was obtained by intramolecular cyclization via photo-induced Diels-Alder reaction in an extremely diluted solution ($3.5 \times 10^{-6} \text{ mol L}^{-1}$). The GPC characterization shows reduced apparent molecular weights of CP2VP ($M_n = 11550$, $\text{PDI} = 1.17$) (Figure S1, Supporting Information, red) in comparison with its linear counterpart, while the MALDI-TOF results demonstrate

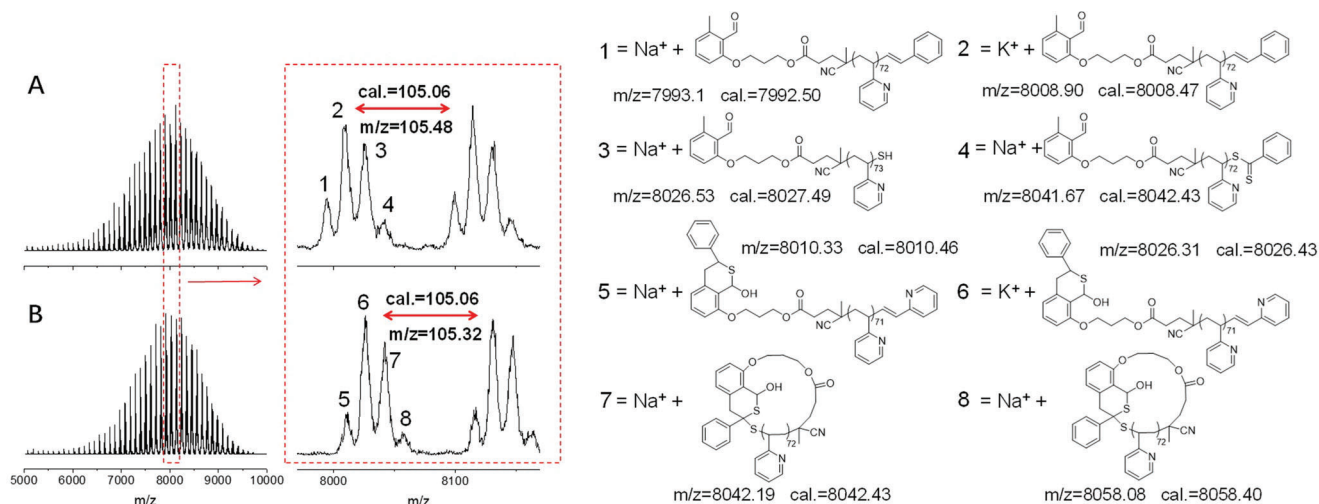


Figure 1. MALDI-TOF mass spectra for LP2VP A) and CP2VP B).

nearly identical data for the absolute molecular weights of LP2VP and CP2VP in the range from 5000 to 10 000 g mol⁻¹ with a peak centered at 8000 g mol⁻¹ (Figure 1). Meanwhile, in their UV-vis spectra the disappearance of the peak at 305 nm ascribing to the thiocarbonyl moiety (Figure S2, Supporting Information) verified the completion of Diels-Alder reaction and successful cyclization of LP2VP into CP2VP. A similar proof is given by the vanishment of the resonance at 10.66 ppm ascribing to the orthoquinodimethane end group in their ¹H NMR spectra for CP2VP (Figure S3, Supporting Information). Subsequently, the linear and cyclic PILs were synthesized by quaternization reaction of LP2VP and CP2VP with BrCH₂CN. The quaternization degrees of linear PILs and cyclic PILs were measured to be 65% and 60%, respectively, calculated by integrating the ¹H NMR spectra (Figure S4A,B, Supporting Information). To further confirm the success of quaternization reactions, the FT-IR spectra were measured for quaternized LP2VP and CP2VP. The production of absorption bands at 1200 cm⁻¹ and 2200 cm⁻¹ in FT-IR spectra (Figure S5, blue) can be ascribed to the newly introduced -CH₂-CN group, in accordance with the ¹H NMR results. Next, anion-exchange was applied to prepare linear and cyclic co-PILs, where the Br⁻ counter anions were only partially exchanged by B(Ph)₄⁻. Accordingly, the B(Ph)₄⁻ anions were chosen as the hydrophobic counter anions because of their bulky aromatic groups.^[24] Besides, the characteristic bands of B(Ph)₄⁻ are clearly seen in the FT-IR spectra (Figure S5, Supporting Information, red), verifying the occurrence of anion-exchange. Ultimately, the exchange efficiency from Br⁻ to B(Ph)₄⁻ is determined to be 77.5% and 84.6% for linear and cyclic co-PILs, respectively, by integrating the corresponding peak areas in the ¹H NMR spectra (Figure S4C,D, Supporting Information). The results indicate that the linear and cyclic co-PILs bear randomly distributed counter anions of Br⁻ and B(Ph)₄⁻ and their chemical structures can be expressed as Lco-PILs([Br⁻]_{0.22}-ran-[B(Ph)₄⁻]_{0.78}) and Cco-PILs([Br⁻]_{0.15}-ran-[B(Ph)₄⁻]_{0.85}), respectively.

Self-assembly of random co-PILs in solution was conducted by dropping water into the as-formed polymer solution in good solvents (DMF or DMSO) with an initial concentration of C_{ini} = 12 mg mL⁻¹. Then, the steady solution with self-assembled

co-PILs was obtained under stirring until water content (C_{H₂O}) reached 90 vol%. By dropping water into the solution of co-PILs, an opaque dispersion formed, indicating that large polymer colloids were obtained and kept stable even without stirring. Afterward, the morphologies of the dispersed polymer colloids were observed by TEM measurements. When using DMF as the good solvent for co-PILs, the morphologies of dispersed colloids were revealed by TEM images as similar spheric particles for Lco-PILs and Cco-PILs (Figure 2). During the assembly process, the movable hydrophobic B(Ph)₄⁻ counter anions aggregated to form the insoluble core of those spheric nanoparticles, minimizing the interfacial interactions between hydrophobic B(Ph)₄⁻ and water.^[21,22] By contrast, the movable hydrophilic Br⁻ counter anions were driven to form the corona of the nanospheres to stabilize the nanoassemblies.^[21,22] Specifically, TEM images of Lco-PILs revealed polydispersed spheric nanoparticles, whose diameter ranges from 40 nm to 300 nm. By contrast, the particle diameter of Cco-PILs ranges from 30 to 160 nm, indicative of reduced nanosphere diameters. Meanwhile, a bimodal distribution with polydispersity index (PDI) of 0.462 in the size range of 30–600 nm was observed by DLS plot for Lco-PILs nanoassemblies (Figure S6A, Supporting Information). Oppositely a monomodal distribution with PDI of 0.091 in the size range of 40–250 nm was observed for Cco-PILs nanoassemblies, which peaks at 100 nm (Figure S6B, Supporting Information). The bimodal distribution of Lco-PILs nanoassemblies and the contrary monomodal distribution of Cco-PILs nanoassemblies in DMF indicate that the cyclic topology has sound influence on the self-assembly of co-PILs. The AFM measurement was further applied to investigate the spheric morphologies of these nanospheres. From the observation of Figure 3A, the large Lco-PILs nanoparticles were measured to show an average width (planar diameter) of 260 nm and a height of 80 nm. In the same AFM setup, the Cco-PILs nanoparticles were measured to show an average width of 120 nm and a height of 40 nm (Figure 3B). Apparently, the size of Cco-PILs nanoassemblies was smaller than the Lco-PILs ones. The obtainment of large self-assembled nanoparticles for Lco-PILs and Cco-PILs can be ascribed to the predominantly hydrophobic segments and minorly hydrophilic segments, because the

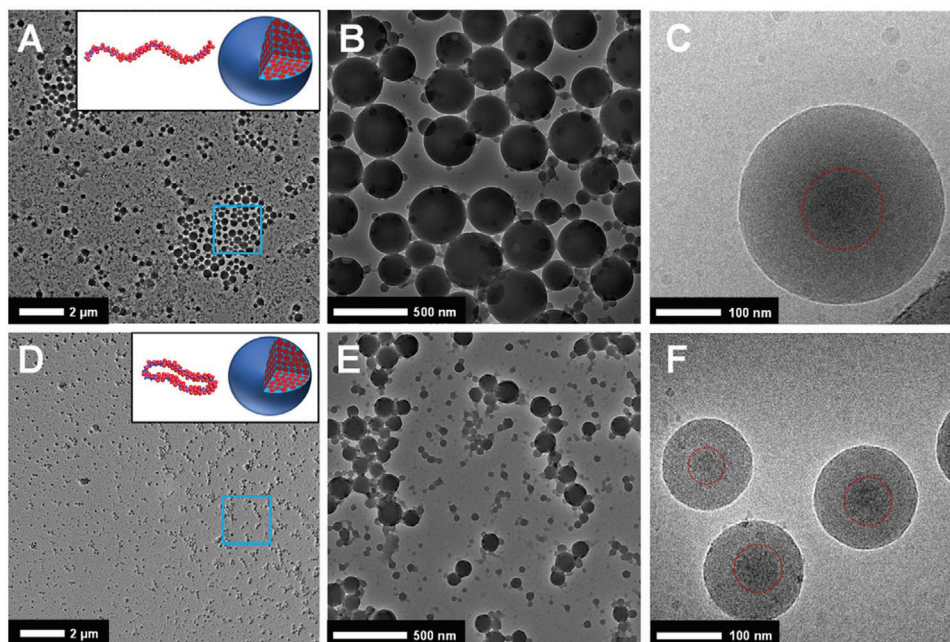


Figure 2. TEM and cryo-TEM images of nanoparticles obtained via the self-assembly of Lco-PILs ($[\text{Br}^-]_{0.22}\text{-ran-}[\text{B}(\text{Ph})_4^-]_{0.78}$) A–C) and Cco-PILs ($[\text{Br}^-]_{0.15}\text{-ran-}[\text{B}(\text{Ph})_4^-]_{0.85}$) D–F) prepared by dropping water into their initial solutions in DMF (12 mg/mL) till a water content of 90 vol.%. The red dotted circles show the higher electron densities derived from a denser distribution of $\text{B}(\text{Ph})_4^-$ in the core (C, F).

hydrophilic segments are too short to balance the elastic and interface energy of the solvophobic segments by solvation so that the relative energy minima can be reached by arrangement to large nanoparticles.^[26–29] To note, no internal structure was observed for these two nanoassemblies by cryo-TEM (Figure 3C,F), and the observed size difference between Lco-PILs and Cco-PILs nanoassemblies in the cryo-TEM survey is in agreement with the results from the TEM analysis.

DMSO was next used as well as the 2nd good solvent to carry out the self-assembly of co-PILs, and its solvent effect was investigated on the co-PILs' self-assembly behaviors. Similarly, the spheric nanoparticles were observed when measuring the samples of Lco-PILs and Cco-PILs by TEM. The sizes of nanoassemblies were measured to be ≈ 50 nm for Lco-PILs and ≈ 30 nm for Cco-PILs, according to the TEM images (Figure S7, Supporting Information). Size distributions of these nanoassemblies were analyzed by DLS (Figure S8, Supporting Information) and exhibited a monomodal size distribution for Lco-PILs and Cco-PILs nanoassemblies, which centered at 45 nm and 25 nm with PDI of 0.105 and 0.072, respectively. The DLS data was in consistence with the TEM results. The smaller diameter range for both Lco-PILs and Cco-PILs nanoassemblies than that obtained in DMF as the starting good solvent, may be ascribed to the different polymer-solvent interaction and the polarity of the solvent, which were reported to have a distinct influence on the self-assembly process.^[26,27,30] Alternatively, the bimodal distribution in DMF but monomodal distribution in DMSO for Lco-PILs nanoassemblies also can be attributed to the difference of polymer-solvent interaction and the polarity of the solvent.^[26,27,30] These data also indicate that the cyclic topology plays indeed a significant role in co-PILs' self-assembly behavior, which may be ascribed to the restriction of co-PILs' chain stretch by the loop.

To get an insight into the experimental results, the self-assembly dynamics of Lco-PILs and Cco-PILs were further investigated by coarse-grain molecular dynamics (CGMD) simulations. As shown in Figures S21–S28, Supporting Information, we conducted self-assembly simulations for both Lco-PILs and Cco-PILs systems with a chain length of 100 and 200 repeating units, respectively. The $\text{B}(\text{Ph})_4^-$ and Br^- ions and P2VP monomer are namely represented by BPh, BR and PVP beads for convenience. The ratio of $\text{B}(\text{Ph})_4^-$ to Br^- in the Lco-PILs systems was 0.22:0.78, and that in the Cco-PILs systems was 0.15:0.85. More details about the simulations can be found in the Supporting Information. As illustrated in **Figure 4**, the statistical radii of Lco-PILs nanoassemblies are larger than Cco-PILs ones, which is consistent with the experimental observations. There are several polymer chains in each nanoassembly for both Lco-PILs or Cco-PILs systems. For the nanoassemblies shown in Figure 4B,E, they contain 24 and 15 polymer chains, respectively. The $\text{B}(\text{Ph})_4^-$ counter anion is away from the surface and the Br^- is relatively enriched on the outside of nanoassemblies with a gradient distribution along the polymer chain. In detail, the radius of gyration of Lco-PILs nanoassemblies ranges from 3.42 nm to 5.68 nm with an average of 4.16 nm. The average number of Lco-PILs nanoassemblies was 8.45, with 1968 coarse-grained beads contained in each nanoassembly on average. As can be seen from the density profiles in Figure S22, Supporting Information, the geometric diameter of the largest Lco-PILs nanoassemblies is approximately 16 nm. By contrast, for the Cco-PILs system, the radius of gyration of the nanoassemblies ranges from 3.19 nm to 4.66 nm with an average of 3.90 nm, and the average number of the Cco-PILs nanoassemblies was 10.00, with 1679 coarse-grained beads contained in each nanoassembly in average. The geometric diameter of the largest Cco-PILs nanoassemblies is ≈ 14 nm.

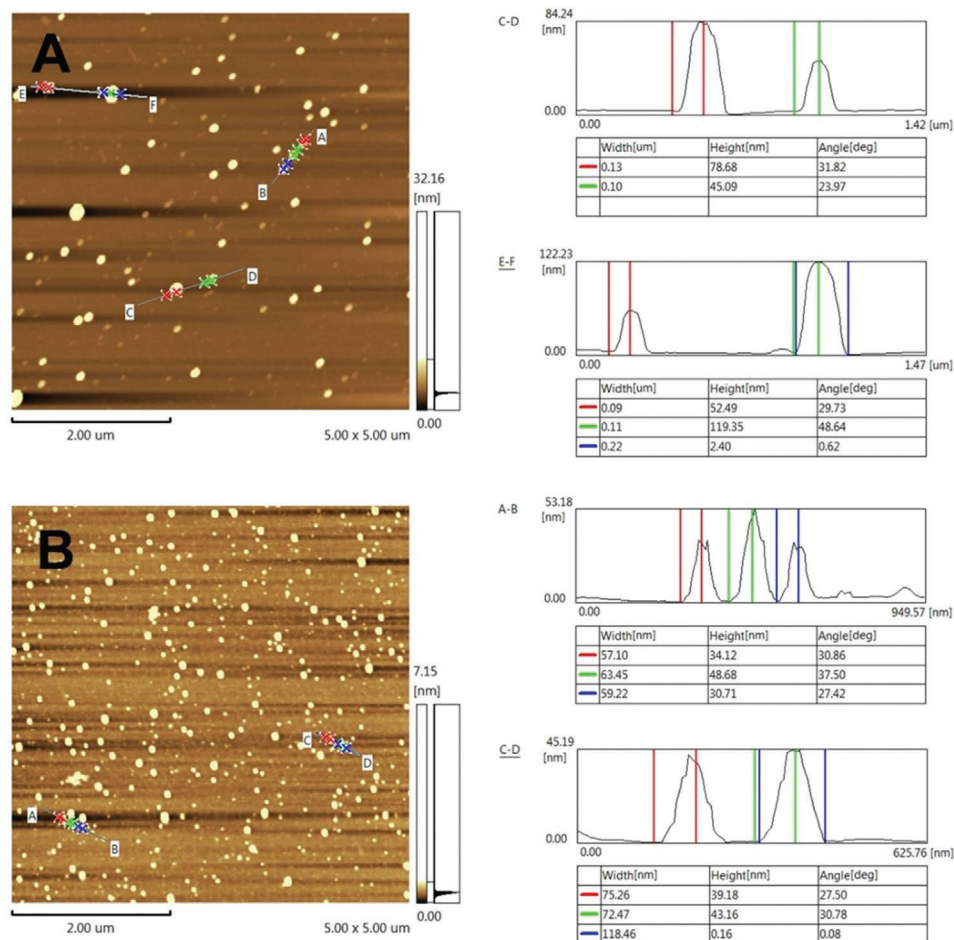


Figure 3. AFM images of nanoparticles obtained via the self-assembly of Lco-PILs ($[\text{Br}^-]_{0.22}\text{-ran-}[\text{B}(\text{Ph})_4^-]_{0.78}$) A) and Cco-PILs ($[\text{Br}^-]_{0.15}\text{-ran-}[\text{B}(\text{Ph})_4^-]_{0.85}$) B) prepared by dropping water into their initial solutions in DMF (12 mg MI^{-1}) till a water content of 90 vol.%.

(Figure S24, Supporting Information). Briefly, the dynamical trend for the self-assembly difference between Lco-PILs and Cco-PILs exhibited by the preliminary results of the CGMD simulations is consistent with that of the experiments, although the specific radii of each system are statistically smaller than the experimental observations, due to the limited simulation time of 960 ns. For self-assembly of amphiphilic diblock copolymers bearing predominantly hydrophobic segments, the spherical aggregates were generally transitioned from spherical micelles.^[26–29] Based on the results of CGMD simulations, we speculate that the spherical aggregates are formed by transitioning from micelles, which formed by enriched hydrophobic counter anions in the core and enriched hydrophilic counter anions in the corona, showing gradient block-like structures (Scheme 1). Such distribution differences of counter anions can be evidenced by the varied contrast of the self-assembled coPIL nanoparticles observed in the Cryo-TEM images (Figure 2C,F). In these nanoparticles, the higher contrast of core areas than corona areas can be ascribed to the higher electron densities derived from denser $\text{B}(\text{Ph})_4^-$ in the core. Generally, the simulation results, despite the variation in resulting dimensions, agreed dynamically and statistically

with the observations in the self-assembly experiments both in size difference as well as in variation tendency for the nanoassemblies.

3. Conclusion

In summary, Lco-PILs and Cco-PILs bearing randomly distributed counter anions of $[\text{Br}^-]$ and $[\text{B}(\text{Ph})_4^-]$ were synthesized by partial counter anion exchange of quaternized linear and cyclic P2VP. The obtained Lco-PILs ($[\text{Br}^-]_{0.22}\text{-ran-}[\text{B}(\text{Ph})_4^-]_{0.78}$) and Cco-PILs ($[\text{Br}^-]_{0.15}\text{-ran-}[\text{B}(\text{Ph})_4^-]_{0.85}$) were self-assembled into nanoparticles in DMF/ H_2O ($v/v = 1/9$) mixture solutions, showing a regulated spheric morphology but multi-dispersed diameters. The Cco-PILs nanoassemblies demonstrated 46% maximum diameter reduce in comparison with the corresponding Lco-PILs nanoassemblies, which may be caused by the restriction of polymer chains' stretch due to their cyclic architecture. Both Lco-PILs and Cco-PILs were found to self-assemble into smaller bulky spheres in DMSO/ H_2O ($v/v = 1/9$) mixture solutions and exhibited similarly a smaller diameter of Cco-PILs nanoparticles than Lco-PILs ones. CGMD simulation shows the tendency of that Lco-PILs nanoassemblies have a larger average

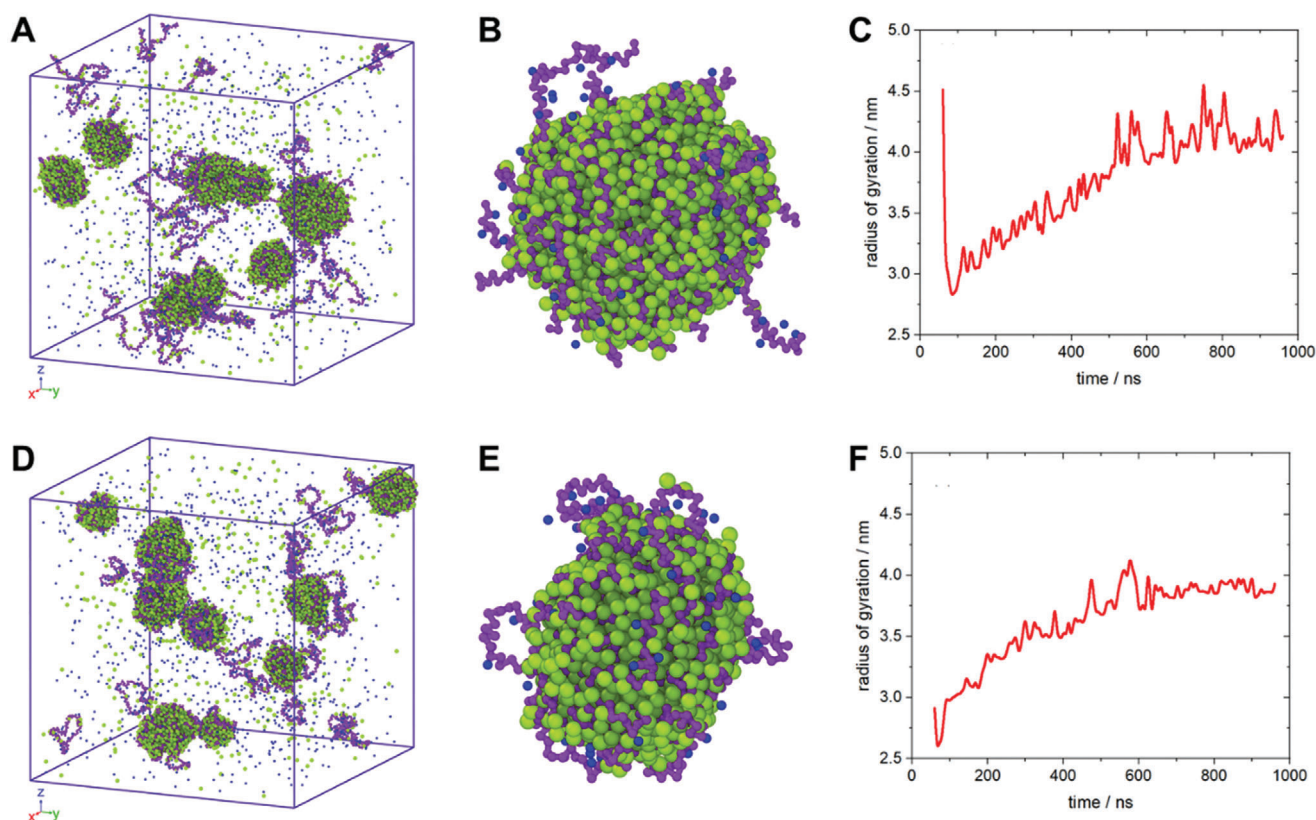


Figure 4. CGMD simulation of self-assembled Lco-PILs ($[\text{Br}^-]_{0.22}\text{-ran-}[\text{B}(\text{Ph})_4^-]_{0.78}$) and Cco-PILs ($[\text{Br}^-]_{0.15}\text{-ran-}[\text{B}(\text{Ph})_4^-]_{0.85}$) nanoparticles. Simulation results of A) Lco-PILs ($[\text{Br}^-]_{0.22}\text{-ran-}[\text{B}(\text{Ph})_4^-]_{0.78}$) and D) Cco-PILs ($[\text{Br}^-]_{0.15}\text{-ran-}[\text{B}(\text{Ph})_4^-]_{0.85}$) with a chain length of 100 beads in the simulated box with a size of $600 \times 600 \times 600 \text{ \AA}^3$. Microstructures of obtained largest single nanoparticle for B) Lco-PILs ($[\text{Br}^-]_{0.22}\text{-ran-}[\text{B}(\text{Ph})_4^-]_{0.78}$) and E) Cco-PILs ($[\text{Br}^-]_{0.15}\text{-ran-}[\text{B}(\text{Ph})_4^-]_{0.85}$) (Purple, chartreuse and blue beads represent polymer chains, $\text{B}(\text{Ph})_4^-$ anions, and Br^- anions, respectively). Evolution of the radius of gyrations for self-assembled C) Lco-PILs ($[\text{Br}^-]_{0.22}\text{-ran-}[\text{B}(\text{Ph})_4^-]_{0.78}$) and F) Cco-PILs ($[\text{Br}^-]_{0.15}\text{-ran-}[\text{B}(\text{Ph})_4^-]_{0.85}$) nanoparticles.

diameter than Cco-PILs nanoassemblies. This work provides a valuable example of self-assembly of cyclic PILs by incorporating randomly distributed counter anions, without involving amphiphilic block structures. The experimental observation and theoretical simulation of cyclic topology on the self-assembly show a size decrease of the obtained spherical nanoparticles in comparison to linear ones, which are believed to benefit the in-depth understanding of the topological effects on the self-assembly behaviors of cyclic PILs.

Supporting Information

Supporting Information is available from the Wiley Online Library or from the author.

Acknowledgements

Generous support was primarily provided by the National Natural Science Foundation of China (22001199, 22102021), the Fundamental Research Funds for the Central Universities (2232022A-03), the Shanghai Pujiang Program (20PJ1400300), and the Natural Science Foundation of Shanghai (21ZR1402700). J.Y. thanks Swedish Research Council Grant 2018-05351 for financial support.

Conflict of Interest

The authors declare no conflict of interest.

Data Availability Statement

The data that support the findings of this study are available in the supplementary material of this article.

Keywords

cyclic polymers, molecular dynamic simulations, nanospheres, poly(ionic liquid), self-assembly

Received: April 28, 2022

Revised: June 24, 2022

Published online:

- [1] W. Qian, J. Texter, F. Yan, *Chem. Soc. Rev.* **2017**, *46*, 1124.
- [2] W. Xu, P. A. Ledin, V. V. Shevchenko, V. V. Tsukruk, *ACS Appl. Mater. Interfaces* **2015**, *7*, 12570.
- [3] J. Kötz, S. Kosmella, T. Beitz, *Prog. Polym. Sci.* **2001**, *26*, 1199.

- [4] S.-Y. Zhang, Q. Zhuang, M. Zhang, H. Wang, Z. Gao, J.-K. Sun, J. Yuan, *Chem. Soc. Rev.* **2020**, 49, 1726.
- [5] W. Zhang, Q. Zhao, J. Yuan, *Angew. Chem., Int. Ed.* **2018**, 57, 6754.
- [6] X. Zhu, C. Wei, H. Chen, C. Zhang, H. Peng, D. Wang, J. Yuan, J. H. Waite, Q. Zhao, *Adv. Funct. Mater.* **2022**, 32, 2105464.
- [7] Y. Ni, X. Zhou, J. Gong, L. Xue, Q. Zhao, *Adv. Funct. Mater.* **2021**, 31, 2103818.
- [8] Y. Zhou, W. Huang, J. Liu, X. Zhu, D. Yan, *Adv. Mater.* **2010**, 22, 4567.
- [9] D. V. Pergushov, I. A. Babin, A. B. Zevin, A. H. Müller, *Polym. Int.* **2013**, 62, 13.
- [10] X. Lin, Q. He, J. Li, *Chem. Soc. Rev.* **2012**, 41, 3584.
- [11] J. E. Poelma, K. Ono, D. Miyajima, T. Aida, K. Satoh, C. J. Hawker, *ACS Nano* **2012**, 6, 10845.
- [12] M. Schappacher, A. Deffieux, *Science* **2008**, 319, 1512.
- [13] B. Zhang, H. Zhang, Y. Li, J. N. Hoskins, S. M. Grayson, *ACS Macro Lett.* **2013**, 2, 845.
- [14] T. Yamamoto, Y. Tezuka, *Soft Matter* **2015**, 11, 7458.
- [15] S. Honda, T. Yamamoto, Y. Tezuka, *J. Am. Chem. Soc.* **2010**, 132, 10251.
- [16] S. Honda, T. Yamamoto, Y. Tezuka, *Nat. Commun.* **2013**, 4, 1574.
- [17] A. V. Dobrynin, R. H. Colby, M. Rubinstein, *Macromolecules* **1995**, 28, 1859.
- [18] A. R. Khokhlov, K. A. Khachaturian, *Polymer* **1982**, 23, 1742.
- [19] H. Yang, Q. Zheng, R. Cheng, *Colloids Surf., A* **2012**, 407, 1.
- [20] Q. Tang, W. Zhang, J. Yuan, Q. Zhao, *React. Funct. Polym.* **2019**, 138, 1.
- [21] J. Guo, Y. Zhou, L. Qiu, C. Yuan, F. Yan, *Polym. Chem.* **2013**, 4, 4004.
- [22] M. Isik, A. M. Fernandes, K. Vijayakrishna, M. Paulis, D. Mecerreyes, *Polym. Chem.* **2016**, 7, 1668.
- [23] M. Ahmed, K.-I. Inoue, S. Nihonyanagi, T. Tahara, *Angew. Chem., Int. Ed.* **2020**, 59, 9498.
- [24] I. Shulov, Y. Arntz, Y. Mély, V. G. Pivovarenko, A. S. Klymchenko, *Chem. Commun.* **2016**, 52, 7962.
- [25] G. M. Whitesides, B. Grzybowski, *Science* **2002**, 295, 2418.
- [26] R. Simonutti, D. Bertani, R. Marotta, S. Ferrario, D. Manzone, M. Mauri, M. Gregori, A. Orlando, M. Masserini, *Polymer* **2021**, 218, 123511.
- [27] Y. Yu, L. Zhang, A. Eisenberg, *Macromolecules* **1998**, 31, 1144.
- [28] E. B. Zhulina, M. Adam, I. Larue, S. S. Sheiko, M. Rubinstein, *Macromolecules* **2005**, 38, 5330.
- [29] C. Chen, M. K. Singh, K. Wunderlich, S. Harvey, C. J. Whitfield, Z. Zhou, M. Wagner, K. Landfester, I. Lieberwirth, G. Fytas, K. Kremer, D. Mukherji, D. Y. W. Ng, T. Weil, *Nat. Commun.* **2021**, 12, 3959.
- [30] Y. Kang, A. Pitto-Barry, M. S. Rolph, Z. Hua, I. Hands-Portman, N. Kirby, R. K. O'reilly, *Polym. Chem.* **2016**, 7, 2836.